The Cytosolic Inactivation Domains of BK_i Channels in Rat Chromaffin Cells Do Not Behave Like Simple, Open-Channel Blockers

C. R. Solaro, J. P. Ding, Z. W. Li, and C. J. Lingle
Washington University School of Medicine, Department of Anesthesiology, St. Louis, Missouri 63110 USA

ABSTRACT Most BK-type voltage- and Ca^{2+}-dependent K^+ channels in rat chromaffin cells exhibit rapid inactivation. This inactivation is abolished by brief trypsin application to the cytosolic face of membrane patches. Here we examine the effects of cytosolic channel blockade and pore occupancy on this inactivation process, using inside-out patches and whole-cell recordings. Occupancy of a superficial pore-blocking site by cytosolic quaternary blockers does not slow inactivation. Occupancy of a deeper pore-blocking site by cytosolic application of Cs^+ is also without effect on the onset of inactivation. Although the rate of inactivation is relatively unaffected by changes in extracellular K^+, the rate of recovery from inactivation (at −80 and −140 mV with 10 μM Ca^{2+}) is faster with increases in extracellular K^+ but is unaffected by the impermeant ion, Na^+. When tail currents are compared after repolarization, either while channels are open or after inactivation, no channel reopening is detectable during recovery from inactivation. BK inactivation appears to be mechanistically distinct from that of other inactivating voltage-dependent channels. Although involving a trypsin-sensitive cytosolic structure, the block to permeation does not appear to occur directly at the cytosolic mouth or inner half of the ion permeation pathway.

INTRODUCTION

Most rat adrenal chromaffin cells express a novel form of large-conductance, calcium (Ca^{2+})- and voltage-dependent K^+ channel that exhibits relatively rapid inactivation (Solaro and Lingle, 1992; Solaro et al., 1995). Inactivation of this channel (termed the BK_i channel) is sensitive to cytosolic trypsin (Solaro and Lingle, 1992), indicating the participation of trypsin-sensitive cytosolic structures. The apparent rate of inactivation exhibits dependence on both membrane depolarization and submembrane [Ca^{2+}] before reaching a limiting value at more positive potentials and higher [Ca^{2+}]. This suggests that inactivation is coupled to structural transitions associated with channel activation (Solaro and Lingle, 1992). BK channels, including the BK_i channel from chromaffin cells, are known to be blocked by the N-terminal ball peptide domain from the *Shaker* B voltage-dependent K^+ channel (Toro et al., 1992; Foster et al., 1992; Solaro and Lingle, 1992). Although these features of BK_i channel behavior are shared with N-terminal type inactivation of voltage-dependent K^+ channels (Hoshi et al., 1990; Zagotta et al., 1990), sensitivity to cytosolic trypsin and coupling of inactivation rate to conditions favoring channel activation are also characteristic of inactivation of other voltage-gated channels, including voltage-dependent Na^+ channels (Rojas and Armstrong, 1971; Gonoi and Hille, 1987). The extent to which BK_i inactivation shares mechanistic similarities to the inactivation of other voltage-dependent channels remains unknown.

Inactivation of voltage-dependent channels can arise from a number of distinct types of cytosolic structures. For voltage-dependent K^+ channels, N-terminal domains of KV1 and KV3 proteins are known to mediate rapid inactivation (Ruppersberg et al., 1991; Rettig et al., 1994; Covarrubias et al., 1994), and, similarly, N-terminal domains of KVβ1 (Rettig et al., 1994) and KVβ3 (Morales et al., 1995; England et al., 1995) subunits mediate a similar type of inactivation. More recently, both C-terminal and N-terminal domains have been shown to contribute to rapid inactivation in a mouse *Shal* channel, although how these domains produce inactivation remains to be defined (Jerng and Covarrubias, 1997). For voltage-dependent Na^+ channels, inactivation is thought to be mediated by a single cytosolic loop connecting the third and fourth cassettes of 6-transmembrane domains (Vassliev et al., 1988; Patton et al., 1993). In each of these cases, it is thought that inactivation involves occlusion of the ion permeation pathway by the inactivation domain.

In contrast to those inactivation mechanisms involving cytosolic structures, some voltage-dependent K^+ channels also undergo a usually slower type of inactivation, sometimes termed C-type inactivation (Hoshi et al., 1991; Lopez-Borneo et al., 1993). C-type inactivation appears to result from the concerted interaction of all subunits in a channel tetramer (Ogielska et al., 1995; Panyi et al., 1995) acting to produce a constriction near the extracellular opening of the pore.

Here we address the issue of the extent to which BK_i inactivation shares mechanistic similarities to inactivation of other voltage-dependent channels. Although the native inactivation process is not sensitive to a number of cytosolic blockers, the rate of recovery from inactivation (but not rate of onset) is sensitive to the presence of extracellular permeant ions. Unlike *Shaker*-type inactivation (Demo and Yellen, 1991; Gomez-Lagunas and Armstrong, 1994), after

Received for publication 12 March 1997 and in final form 15 May 1997.
Address reprint requests to Dr. Chris Lingle, Department of Anesthesiology, Washington University School of Medicine, 660 S. Euclid Ave., St. Louis, MO 63110. Tel.: 314-362-8558; Fax: 314-362-8571; E-mail: clingle@morpheus.wustl.edu.

0006-3495/97/08/819/12 $2.00

inactivation, channels recover from inactivation without appreciable passage through open states. Thus, in contrast to N-terminal inactivation of voltage-dependent K^+ channels, the results suggest that the native inactivation domain does not interact directly with the intracellular mouth of the BK channel. These results suggest that BK_i inactivation is mechanistically distinct from all previously described inactivation mechanisms.

MATERIALS AND METHODS

Chromaffin cell culture

Methods of rat chromaffin cell isolation and maintenance of cultures were as described previously (Neely and Lingle, 1992; Herrington et al., 1995; Solaro et al., 1995). Chromaffin cell dispersions were typically done on adrenal medullas from three or four rats ~2–3 months age, and currents were recorded 2–12 days after plating.

Electrophysiological methods

Whole-cell and single-channel currents were recorded with standard techniques (Hamill et al., 1981) as described previously (Solaro and Lingle, 1992; Solaro et al., 1995), unless noted otherwise. In whole-cell experiments, uncompensated series resistance (R_s) was typically 1.5–5 MΩ, of which 80–95% was electronically compensated. In most cases, residual uncompensated R_s was less than 1 MΩ. Values for R_s and the percentage compensation for specific experiments are provided in the figure legends.

Ensemble average currents were generated either from the average of raw currents or after idealization of single-channel openings by using a half-amplitude detection procedure. Idealizations of current traces obtained in 0 Ca^{2+} were used to digitally subtract leak and capacity currents from each trace before channel detection. Ensemble average currents generated from either idealized openings or raw currents yielded essentially identical results. Sampling periods were 50–400 μs, and currents were typically acquired with a bandwidth of 5 kHz. For experiments in which channel reopening was examined during recovery from inactivation, the sampling interval was usually 50 μs at a bandwidth of 5 kHz. Current integrals during the recovery periods were calculated digitally from the ensemble current averages.

Analysis of whole-cell and single-channel currents was done either with Clampfit (Axon Instruments, Foster City, CA) or with our own software. For analysis of blocking gaps in the presence of BP, the sampling period for single-channel analysis was 100 μs. Opening and closing transitions were detected with a half-amplitude detection procedure and histograms were generated. All fitting was done with a Levenberg-Marquardt search algorithm to obtain nonlinear least-squares estimates of function parameters. For each closed interval component, the frequency of occurrence of that component was calculated per millisecond of open time (determined from the open interval histogram) for both control and BP conditions. Estimates of the probability of being open within a burst of openings and closings before inactivation were also made from the interval histograms. No attempt was made to correct for missed events.

Predictions for the tail current that would arise from the requirement that inactivated channels must recover through open states were generated with Mathcad 6.0 for Windows (MathSoft, Cambridge, MA).

Solutions

The usual extracellular solution contained the following (in mM): 150 NaCl; 5.4 KCl; 10 HEPES; 1.8 $CaCl_2$, and 2.0 $MgCl_2$, pH 7.4, adjusted with *N*-methylglucamine (NMG). Apamin (200 nM) was added to block SK currents (Neely and Lingle, 1992). For whole-cell recording, the pipette solution contained the following (in mM): 160 KCl, 10 mM HEDTA with added Ca^{2+} to make 10 μM free Ca^{2+}, as defined by the EGTAETC program (E. McCleskey, Vollum Institute). In some cases, intracellular KCl was reduced with equimolar substitution of NaCl and/or CsCl to reduce the magnitude of BK current (Yellen, 1984). Osmolarity was measured by dew point (Wescor Osmometer) and adjusted to within 3% (internal saline, 290; external saline, 305). For experiments with different extracellular $[K^+]$, NaCl was replaced by equimolar substitution with KCl. Tetrodotoxin (200 nM) was used to reduce voltage-dependent Na^+ current. 4-Aminopyridine (1 mM) was routinely included in extracellular salines to completely block a rapidly inactivating voltage-dependent K^+ current. For whole-cell recordings, no correction was made for the +3 mV liquid junction potential that arose with the chloride-based, 10 μM $[Ca^{2+}]$ pipette saline.

For single-channel recordings, cells were initially bathed in the extracellular saline used for whole-cell recordings described above. After seal formation and just before patch excision, the solution bathing the cell was changed to a 0 Ca^{2+} saline described below. For inside-out single-channel recordings, the pipette saline contained (in mM) 140 KCl, 20 KOH, 2 $MgCl_2$, 10 HEPES, pH 7.0 (adjusted with 1 N HCl), and 200 nM apamin. The cytosolic saline used during excised inside-out patch recordings contained the following (in mM): 140 KCl, 20 KOH, 10 HEPES. For solutions containing 2 μM free Ca^{2+}, 5 mM EGTA was included, and $CaCl_2$ was added to make the desired free $[Ca^{2+}]$. For 10 μM free Ca^{2+}, *N*-hydroxyethylethylene-diaminetriacetic acid (HEDTA) was used to buffer Ca^{2+}. In each case, the pH was adjusted to 7.0. Estimates of free $[Ca^{2+}]$ were determined as described previously (Solaro and Lingle, 1992; Herrington et al., 1995). Tetraethylammonium ion (TEA), QX-314, decamethonium, chlorisondamine, leupeptin, and *Shaker* B N-terminal ball peptide (BP) were added directly to the intracellular saline. When used, Cs^+ was added directly to the normal 10 μM Ca^{2+} solution. With solutions containing Cs^+, K^+ was kept at 160 mM to maintain symmetrical K^+ gradients.

Solution exchange and drug applications were accomplished as described previously (Herrington et al., 1995). Chemicals were from Aldrich or Sigma. One preparation of *Shaker* B ball peptide was generously provided by R. Murrell-Lagnado and R. Aldrich (Stanford University). Ball peptide was also obtained from Beckman Lab (Stanford, CA), and the Protein Chemistry Lab, Washington University School of Medicine (St. Louis, MO).

Molecular dimensions

Estimates of the largest distance between any two atoms in a molecule were made with CS Chem3D (CambridgeSoft Corp., Cambridge, MA), after energy minimization of the structure based on the MM2 Force Field. This minimization does not consider interactions with solvent.

RESULTS

Cytosolic blockers of BK current do not compete with the native inactivation process

The ability of small cytosolic channel blockers such as TEA to impede N-terminal inactivation of the *Shaker* B channel suggests that the *Shaker* N-terminal inactivation domains bind to sites sufficiently close to or within the mouth of the ion permeation pathway that they either sterically or electrostatically sense the presence of blocking molecules in sites within the electric field of the channel (Choi et al., 1991; Demo and Yellen, 1991). In contrast, cytosolic TEA, despite producing fast block of BK channels, has no effect on the time course of BK_i inactivation (Lingle et al., 1996). However, it seemed possible that, in contrast to the blockade of *Shaker* channels, the blocking position for TEA

might be sufficiently deep within the BK channel to minimize interaction with a structure occluding the mouth of the channel. We therefore examined a more extensive series of cytosolic blockers. Concentrations of blockers were chosen to result in a ~30–70% reduction in ensemble BK current. As shown in Fig. 1 *A*, 2 mM QX-314 results in no discernible slowing of BK current inactivation, despite producing a ~50% reduction in average current. QX-314 results in a marked reduction in the resolvable single-channel current (Fig. 1 *A*, *inset*), which is known to be voltage dependent (Oda et al., 1992). Similarly, 50 μM decamethonium (Fig. 1 *B*), 20 μM chlorisondamine (Fig. 1 *C*), 300 μM leupeptin (acetyl-leucyl-leucyl-argininal) (Fig. 1 *D*), and 7 and 15 μM curare were without effect on τ_i. At +60 mV, decamethonium, chlorisondamine, and leupeptin all produce a rapid, flickery block of BK channels (Fig. 1, *insets*). Values for percentage block and prolongation in each case are summarized in Table 1.

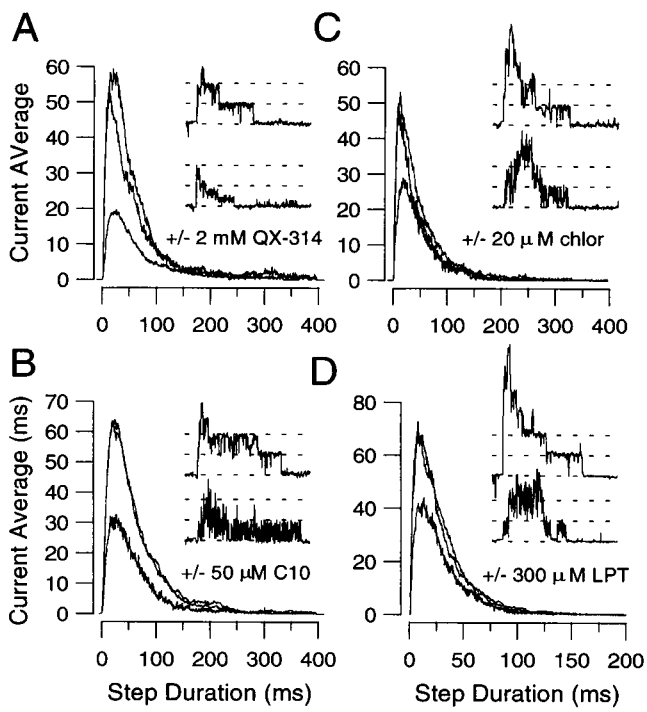

FIGURE 1 Cytosolic channel blockers of BK channels do not impede the BK_i inactivation process. BK_i currents were activated in inside-out patches by depolarizing voltages steps to +60 mV after brief steps to −140 mV in the constant presence of 10 μM Ca^{2+}. Sample currents activated by single voltage steps are shown for each patch for both saline with 10 μM Ca^{2+} (*top traces*) and 10 μM Ca^{2+} plus blocker (*bottom traces*). Ensemble average currents were generated from the idealized channel openings from at least 30 separate voltage steps. For each blocker, no indication of a slowing of inactivation was observed. (*A*) Currents were elicited in the absence and presence of 2 mM QX-314 (nine-channel patch; control: 40.4 ms; QX-314; 43.4 ms; recovery: 44.8 ms). (*B*) Currents from the same patch as in *A* with and without 50 μM decamethonium (C10) (control: 47.8 ms; C10: 38.3 ms; recovery: 45.6 ms). (*C*) Currents with and without 20 μM chlorisondamine (six-channel patch; control: 44.8 ms; chlor: 40.6 ms; recovery: 40.0 ms). (*D*) Currents with and without 300 μM leupeptin (10-channel patch; control: 26.1 ms; LPT: 25.6 ms; recovery: 25.6 ms). (*Insets*) 200-ms traces in *A–C* and 100-ms traces in *D*. Dotted lines are separated by 15 pA.

For the slowing of inactivation of *Shaker* B K^+ channels by TEA, the blocking action of TEA was analyzed from the viewpoint of a simple block scheme, in which open channels can be either blocked or inactivate (Choi et al., 1991). In accordance with this scheme, if transitions into and out of the blocked state are sufficiently rapid relative to the rate of entry into the inactivated state, macroscopic current decay will be prolonged by a factor identical to the fractional reduction in peak current amplitude (Choi et al., 1991). For blocking reactions in which the duration of the blocked state is long compared to the rising phase of current activation, the predictions are not as simple, but the decay of the current will be expected to contain at least one component that will be slower than the normal inactivation time course. For those compounds examined here, blockade by QX-314 results in a reduction in the single-channel current, indicating that it meets the criteria for a fast blocker. Decamethonium has been shown to block skeletal muscle BK channels with a 0-voltage K_d of 43 μM (Villarroel et al., 1988), generally consistent with the amount of block observed here. Assuming forward blocking rates of $\sim 10^7\ M^{-1}\ s^{-1}$, this would imply that any open channel will undergo several cycles of block and unblock during the rising phase of the ensemble currents observed here. This is consistent with the frequent, brief blocked events observed in both the traces with decamethonium and chlorisondamine. For leupeptin, the blocking affinity is even weaker, implying even more rapid blocking kinetics. Single-channel openings with leupeptin lack resolved closures and exhibit a noisy current level intermediate between the fully open and fully closed conditions. Thus, qualitatively, each of these blockers meets the criterion that the blocking reactions are relatively fast compared to the intrinsic time course of inactivation. Furthermore, none of the averaged currents in the presence of these blocking drugs exhibited a component of decay slower than the normal inactivation time course. These results, therefore, allow us to infer that none of these compounds impede the movement of the native inactivation domain during the inactivation process.

Although a detailed analysis of blocking mechanisms has not been made here, decamethonium is known to produce a voltage-dependent block of BK channels (Villarroel et al., 1988). Furthermore, with both chlorisondamine and leupeptin, the fast blocking events seen at positive potentials are not discernible in BK openings at negative potentials. In addition, neither QX-314, decamethonium, nor chlorisondamine reduces BK tail current amplitudes at potentials of −40 mV or more negative (not shown), indicating that block is rapidly removed upon repolarization. Qualitatively, the voltage dependence of these blocking effects argues that these agents act as channel blockers binding within the ion permeation pathway. Thus we conclude that the native inactivation process is not impeded by occupancy of the cytosolic mouth of the BK channel by a number of open channel blockers.

TABLE 1 Effect of cytosolic BK channel blockers on prolongation of τ_i

[Drug]	% Block Mean ± SD	τ_d/τ_c Mean ± SD	Applications	Patches	Length* (Å)
2 mM QX314	57.7 ± 10.4	1.06 ± 0.11	10	9	12.27
20 μM chlor	32.5 ± 12.5	1.16 ± 0.36	7	5	9.08
50 μM C10	52.1 ± 8.7	1.04 ± 0.21	5	5	18.37#
300 μM LPT	33.6 ± 3.7	1.04 ± 0.05	3	1	17.51
7 μM curare	34.5 ± 1.21	1.21 ± 0.08	3	3	16.87
15 μM curare	69.3 ± 3.3	1.20 ± 0.13	6	4	

*Length between two most distant atoms estimated from CS Chem3D.
#This represents an extended C10 conformation.

The *Shaker* B BP does not compete with the normal inactivation process. Removal of the inactivation process does not alter sensitivity to BP

We next examined the ability of the 22 amino-acid N-terminal *Shaker* B peptide (BP) to compete with BK_i inactivation. BP blocks BK channels at a site that is competitive with TEA (Toro et al., 1992; Foster et al., 1992), implying that the BP interacts with a site sensitive to occupancy of the channel by TEA. Furthermore, block of cloned mSlo channels by BP is of sufficiently low affinity that, at concentrations that produce appreciable block of BK current, the blocking equilibrium is largely complete during the rising phase of BK current activated by voltage steps (Lingle et al., 1996). The kinetics of the blocking process itself will therefore be well separated from the rates of channel inactivation. This allows the prediction that, if BP occupies a site that slows the movement of a native inactivation structure to its blocking position, there will be a component of current relaxation that will be slower than the normal current inactivation rate.

The rapid blocking effect of BP on BK_i channels is shown in Fig. 2 *A* for a single-channel patch. A BP concentration of 600 μM results in a marked increase in brief closing events. Ensemble average currents show that BP produces a minimal effect on τ_i. Whereas a small prolongation of τ_i was observed in the example shown with 400 μM BP (Fig. 2 *B*), no change was observed with 600 μM BP. Because a small number of bursts were used for the ensemble average currents for this patch, some variability in τ_i is not unexpected. In patches with a larger number of BK_i channels, the inability of BP to alter τ_i could be more clearly seen (Fig. 2 *C*). Fig. 2 *C* also displays the predicted prolongation of current averages based on the simple competition model (Choi et al., 1991) for either 50% reduction of current (twofold prolongation of decay) and for the observed amount of reduction (~70%; 3.4-fold prolongation). From experiments utilizing two preparations of BP, the ratio of control current amplitude (I_C) to current amplitude in the presence of BP (I_{BP}) was determined along with the fractional prolongation of τ_i by BP ($\tau_i(BP)/\tau_i(C)$). Estimates using either 400 μM or 600 μM BP were averaged and are plotted in Fig. 2 *D*. Whereas a simple competition model predicts that the two ratios should vary with a slope of 1, τ_i was unaffected by BP.

That the BP blocking reaction is sufficiently rapid to be considered near steady-state at the peak of the ensemble average current was also verified by analysis of the single-channel patch shown in Fig. 2 *A*. At +60 mV, in comparison to control channel activity, 400 μM BP was associated with two components in the closed interval distributions: one of ~0.77 ms occurring with a frequency of 0.79/ms open time, and a second of ~5.7 ms with a frequency of 0.16/ms open time (data not shown). Thus an open BK channel will, on average, undergo several cycles of block and unblock during the ~10-ms rising phase of the average current. As a consequence, fractional block of peak ensemble current is a reasonable approximation of the steady-state block by BP. This is also supported by the fact that the probability of being open, calculated from the durations of all openings and closures within bursts, was 0.876 for control bursts and 0.375 for bursts in 400 μM BP. Steady-state block by 400 μM BP calculated from these values is therefore ~57%, which is comparable to what is observed in Fig. 2 *B* from the peak of the ensemble current average. Thus BP blocking reaction is rapid enough that, if BP were hindering the native inactivation process, it would clearly appear as a prolongation of the normal apparent inactivation process. This is not observed.

Failure to observe competition by BP might also occur if there were a slow component of block by BP, such that after some number of rapid blocking events, BK channels entered a long-lived blocked state at a rate comparable to the normal inactivation rate. Although two blocking gaps resulting from BP action on BK channels have been described (Foster et al., 1992; Toro et al., 1992), the frequency of occurrence of the longer blocking gap in those studies does not appear to have the characteristics required to mimic inactivation. Furthermore, if the inactivation rate with BP reflected a slow blocking effect of BP, the apparent inactivation rate should increase as [BP] increases. This is not observed. A direct test of this possibility is shown in Fig. 2 *E*. After removal of inactivation in a patch with BK_i channels by trypsin, 400 μM BP results in fast block of BK current with no slow block component. Thus we conclude that the lack of effect of BP on the normal inactivation time course results

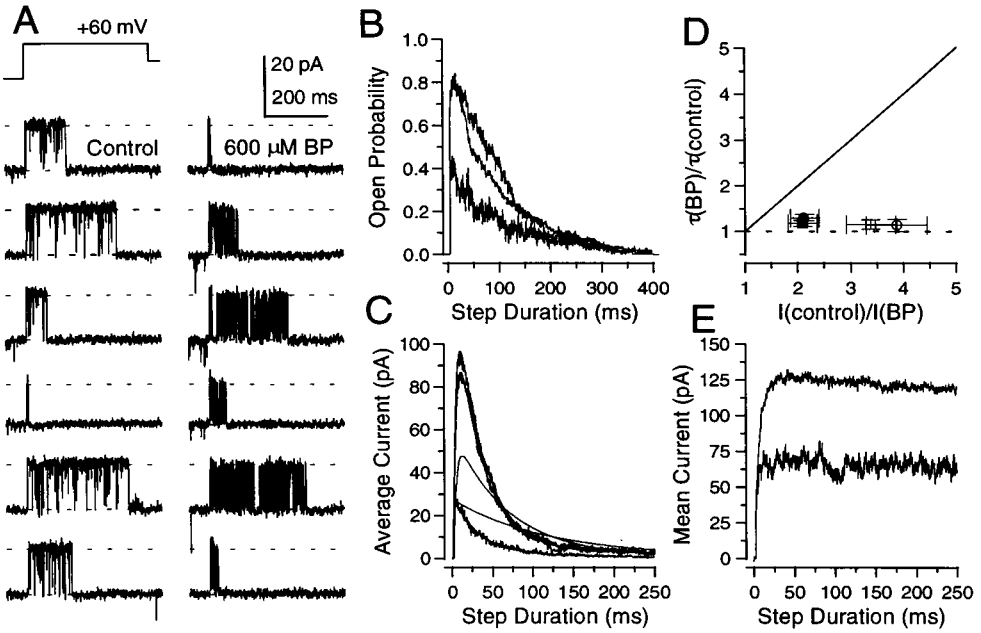

FIGURE 2 Blockade of BK_i channels by the *Shaker* B BP does not impede the BK_i inactivation process. (*A*) BK_i openings from a single-channel patch in the absence and presence of 600 μM BP. Openings were activated by steps to +60 mV from −140 mV with 10 μM Ca^{2+}. In each column all traces were consecutive. BP results in a large increase in short-duration closures. (*B*) Ensemble currents from the same patch as in *A*, but traces with and without 400 μM BP are shown. BP has little effect on either the time constant of inactivation (τ_i) or the likelihood that a channel will open during a sweep. τ_i for control, 400 μM BP, and recovery ensembles were 97.6, 118.3, and 99.6 ms; τ_i for control, 600 μM BP, and recovery ensembles were 135.0, 118, and 113.1 ms. (*C*) Ensembles of single-channel idealizations from a patch with nine BK_i channels. 400 μM BP resulted in a ~71% reduction of peak BK_i current with no discernible change in time constant (control: 33.8 ms; BP: 33.7 ms: recovery: 32.7 ms). Fitted activation/inactivation waveforms are laid over the average currents. The solid lines show the predictions for a simple competition model between BP and the inactivation process for 50% reduction of peak current (τ_i = 67.4 ms) and for a 71% reduction in peak current with a 3.4-fold prolongation (τ_i = 114.9 ms). There is a clear absence of late openings in the presence of BP, which is inconsistent with the simple competition model. In *D*, the fractional prolongation of time constants observed with BP is related to the reciprocal of the fractional reduction of BK_i current amplitude produced by BP. The simple competition model predicts the line with a slope of 1, whereas no interaction predicts the dotted line with 0 slope. The filled symbols (12 applications to 10 patches) correspond to estimates of percentage block and time constants with 400 μM BP, and open symbols (four applications to four patches) to estimates with 600 μM BP. Circles correspond to comparisons between currents in BP and before BP application, and squares correspond to comparisons on washout of BP. (*E*) The relative block produced by 400 μM BP after removal of inactivation by trypsin. After trypsin was used to remove inactivation, the patch was exposed to 10 μM Ca^{2+} alone for 25 s, before application of BP. The fractional block by BP is comparable to that when the inactivation mechanism is intact. BP by itself does not produce any slow component of block.

from an inability of BP to compete with the intrinsic inactivation domains. Furthermore, disruption of the native inactivation process by trypsin does not alter the sensitivity of the BK_i channel to blockade by BP.

Internal blockade by Cs^+ does not affect inactivation onset or recovery

The BK channel pore is thought to contain a number of ion-binding sites (Neyton and Miller, 1988a,b; Neyton and Pelleschi, 1991). We therefore wished to address the possibility that the barrier to permeation arising during BK_i inactivation may occur deeper within the pore than the TEA blocking site. Whereas TEA and other quaternary blockers have been proposed to bind about 10 Å within the channel at an electrical distance of ~0.2 (Villarroel et al., 1988, but see Yellen, 1984), Cs^+ also blocks BK channels from the cytosolic side, in accordance with a single-site blocking model with the blocking site located at an electrical depth of ~0.54 (Cecchi et al., 1987; but see Yellen, 1984). Blockade by Cs^+ results from fast channel block with a reduction in single-channel current.

The effect of Cs^+ on the onset of inactivation is summarized in Fig. 3. Cs^+ reduced peak ensemble average current in a concentration-dependent fashion, without producing any appreciable effect on the time course of inactivation. The amount of reduction by Cs^+ of the peak ensemble current is generally consistent with the expected effects of Cs^+ on BK single-channel current (Cecchi et al., 1987). Thus, even at concentrations of Cs^+ in which the channel is occupied over half the time by Cs^+, there is no indication that the native inactivation process is altered.

Rates of recovery from inactivation but not inactivation onset are sensitive to extracellular permeant ions

The ability of some extracellular ions (Demo and Yellen, 1991; Gomez-Lagunas and Armstrong, 1994) to alter the affinity of the *Shaker* N-terminal inactivation domain for its

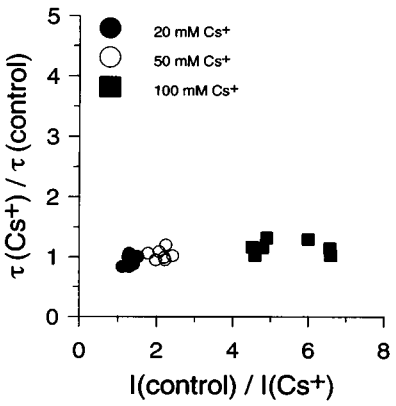

FIGURE 3 Internal block by Cs^+ does not alter the BK_i inactivation rate. Ensemble average currents were elicited as in Fig. 1, with depolarizing steps to +60 mV after brief hyperpolarizations to −140 mV. Submembrane Ca^{2+} was 10 μM. Inactivation time constants (τ) and amplitudes of inactivating current (I) were measured for control, in the presence of 20, 50, or 100 mM Cs^+, and after return to Cs^+-free saline. For each Cs^+ application, the effect of Cs^+ on either τ_i or I was compared to the average of pre- and post-Cs^+ values. The relative changes in inactivation time constant ($\tau(Cs^+)/\tau(control)$) are plotted versus the relative reduction in inactivating current ($I(control)/I(Cs^+)$). The lack of slope in the relationship indicates that Cs^+ has no effect on the inactivation rate.

blocking site has been used to argue that inactivation domains interact closely with the ion permeation pathway. However, the ability of extracellular ions to affect inactivation does not exclude the possibility that occupancy of the permeation pathway by an ion may simply favor a channel conformation less favorable to BP binding (e.g., Demo and Yellen, 1992; Neyton and Miller, 1988b; Neyton and Pelleschi, 1991). Furthermore, recovery from C-type inactivation is also favored by increases in extracellular permeant ions (Levy and Deutsch, 1996). Irrespective of the possible interpretation of the effects of extracellular K^+ on inactivation processes, we wished to determine whether BK_i inactivation was sensitive to the concentration of extracellular K^+. Therefore, BK_i currents were examined in whole-cell recordings in which the pipette solution contained 10 μM Ca^{2+} (Prakriya et al., 1996). This allowed more reliable determination of rates of recovery from inactivation at different voltages and Ca^{2+} than could be accomplished by generation of ensemble currents in inside-out patches.

At potentials positive to 0 mV, the rate of inactivation exhibits a single-exponential component and is dependent on both [Ca^{2+}] and membrane potential up to a limiting value (Solaro and Lingle, 1992; Prakriya et al., 1996). To examine the effects of changes in extracellular K^+, whole-cell BK currents were activated by steps to +90 mV with 10 μM cytosolic Ca^{2+}. For a set of eight cells, the inactivation time constants were 30.9 ± 2.6 ms (mean and SD) at 5.4 mM K^+ and 35.7 ± 2.2 ms with 150 mM $[K^+]_o$. Although the limiting rate of current inactivation at +90 mV appears relatively insensitive to $[K^+]_o$, BK current appeared to activate more rapidly with more elevated extracellular K^+.

Recovery from inactivation at potentials of −40 mV and more negative exhibits two kinetic components (Herrington et al., 1995), with both components exhibiting Ca^{2+} and voltage dependence (Ding et al., 1996). Here, recovery from inactivation was examined with 10 μM cytosolic Ca^{2+}, using either of two different pulse protocols. In one, a standard paired pulse protocol was employed, in which the recovery time between test steps was varied. In the second, a series of steps to +90 mV were separated by increasingly long periods at the recovery potential. The two protocols yield identical estimates of recovery rate (k_r) (Ding et al., 1996), but the shorter duration of the second protocol better maintains cell viability. Fig. 4 *A* shows examples of the currents activated by the second protocol for 5.4 and 150 mM $[K^+]_o$, with recovery at −80 mV. The fractional recovery for these cases as a function of recovery interval is plotted in Fig. 4 *B*. Here, to compare effects of $[K^+]_o$, we have simply fit the recovery time course in each case with a single-exponential function. With 150 mM K^+, k_r is ~25/s at −80 mV, whereas, at 5.4 mM K^+, k_r is ~11.9/s at −80 mV.

The dependence of k_r on $[K^+]_o$ is plotted in Fig. 4 *C* for −140 mV and −80 mV, and Fig. 4 *D* replots the same data to show the voltage dependence of k_r at different $[K^+]_o$. The EC_{50} values for the effect of K^+ on recovery rate are 111.7 ± 52.7 mM at −140 mV, and 111.3 ± 33.4 mM at −80 mV. At −140 mV, $k_r(0)$ was 28.1 ± 4.4/s, whereas $k_r(max)$ was 149.6 ± 21.8/s. At −80 mV, $k_r(0)$ was 15.5/s, whereas $k_r(max)$ was 39.8 ± 2.8/s. There is some indication that voltage dependence is somewhat reduced at lower $[K^+]_o$ (Fig. 4 *D*).

If the effect of $[K^+]_o$ results from an increased likelihood that sites within the channel pore are occupied by an ion, it would be expected that impermeant ions would not affect k_r. To address this, k_r was measured as a function of $[Na^+]_o$. As illustrated in Fig. 4 *E*, k_r is only slightly faster at 150 mM than at 0 mM $[Na^+]_o$. The voltage dependence of k_r remains similar at all $[Na^+]_o$. k_r was similar in 0 Na^+, 0 K^+, irrespective of whether 150 mM NMG, 285 mM sucrose, or 170 mM Tris was used in the extracellular saline (Fig. 4 *F*). These experiments again suggest that the voltage dependence of recovery is reduced in the absence of extracellular permeant ions, but that some voltage dependence remains.

Recovery from inactivation occurs without appreciable passage through open states

Recovery from inactivation of some voltage-dependent K^+ channels is associated with a slow tail of channel reopenings (Demo and Yellen, 1991; Ruppersberg et al., 1991; Gomez-Lagunas and Armstrong, 1995). This is presumed to indicate that occupancy of the channel by the inactivation domain hinders channel closure such that, most of the time, but not always, such channels must recover from inactivation by first passing through the open state. However, preliminary experiments suggested that recovery from inactivation of BK_i channels does not require channel reopening (Lingle et al., 1996). Specifically, in patches with few BK

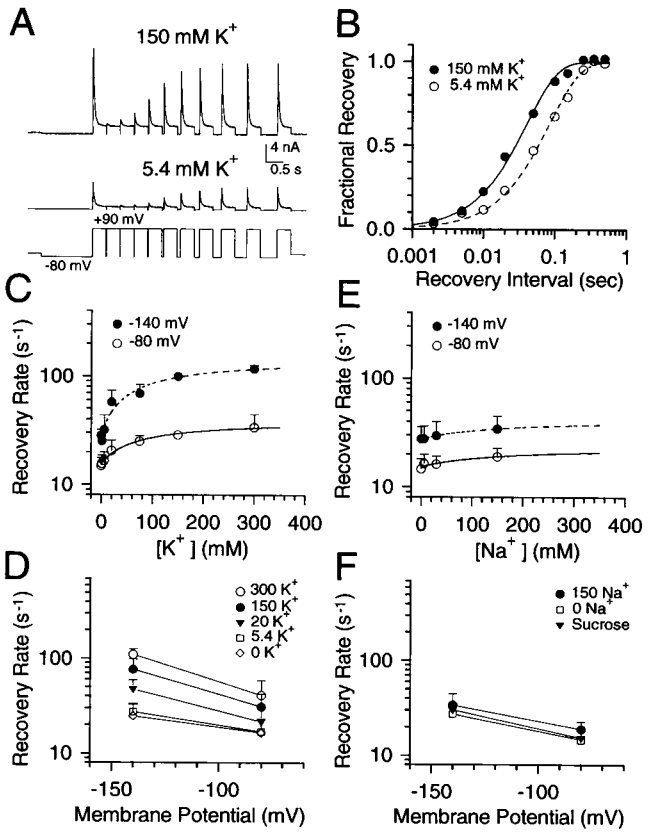

FIGURE 4 The rate of recovery from inactivation is faster with increased $[K^+]_o$. Whole-cell BK currents were recorded with 10 μM pipette Ca^{2+}. The recovery from inactivation was examined by using a sequential pulse protocol of 200-ms steps to +90 mV, which were separated by variable recovery intervals (1 ms to 2 s) at different recovery potentials. (*A*) Representative currents generated using this protocol are shown for a recovery potential of −80 mV for both 5.4 mM (*bottom*) or 150 mM $[K^+]_o$ (R_s:4.6 mΩ; C_m:8.5 pF; 80% compensation). (*B*) The fractional recovery is plotted as a function of recovery duration for the currents in *A* obtained at −80 mV, qualitatively showing the shift to faster recovery at more elevated extracellular $[K^+]$ [τ_r = 84 ms at 5.4 mM (○) and 40 ms at 150 mM (●)]. (*C*) The recovery rate at −140 (●) and −80 mV (○) as a function of extracellular K^+ is plotted. Error bars are standard deviations. The lines are fits of the function (Murrell-Lagnado and Aldrich, 1993): $k_r = P(\text{occ.})\,k_r(0) + [1 - P(\text{occ.})]k_r(\text{max})$ (2), where $P(\text{occ.}) = 1/(1 + K_d/[K^+]_o)$ and K_d representing an apparent K^+ dissociation constant. Resulting values are provided in the text. For K^+ below 150 mM, NMG was added to maintain osmolarity near 300. (*D*) The same points are replotted to show that there is minimal change in the voltage dependence of the apparent recovery rate from 0 to high K^+. (*E*) Apparent recovery rates are plotted as a function of Na^+ at −140 mV (●) and at −80 mV (○). As in *C*, NMG was used to maintain osmolarity. (*F*) Apparent recovery rates for cells with 150 mM Na^+_o, or with 0 Na/0 K with either NMG or sucrose are plotted for −80 and −140 mV. All conditions with 0 external permeant ions yield similar values, and retain a voltage dependence slightly reduced relative to that observed with elevated extracellular K^+.

channels, the current integral generated from idealizations of openings detected during deactivation of open channels greatly exceeded the current integral obtained during recovery from inactivation. Because of concern that the detection process might in some way bias the result, here we have examined this issue in more detail, using patches with larger numbers of channels.

Fig. 5 *A* provides an example of the stimulation protocol and resulting ensemble average current for this type of experiment. For this set of experiments, current was activated with 10 μM Ca^{2+}. The protocol was designed to compare the tail of current after repolarization to −140 from +60 for two cases: first, when most channels are open at +60 mV and, second, when all channels are inactivated at +60 mV. To accomplish this, an initial 100-ms step to

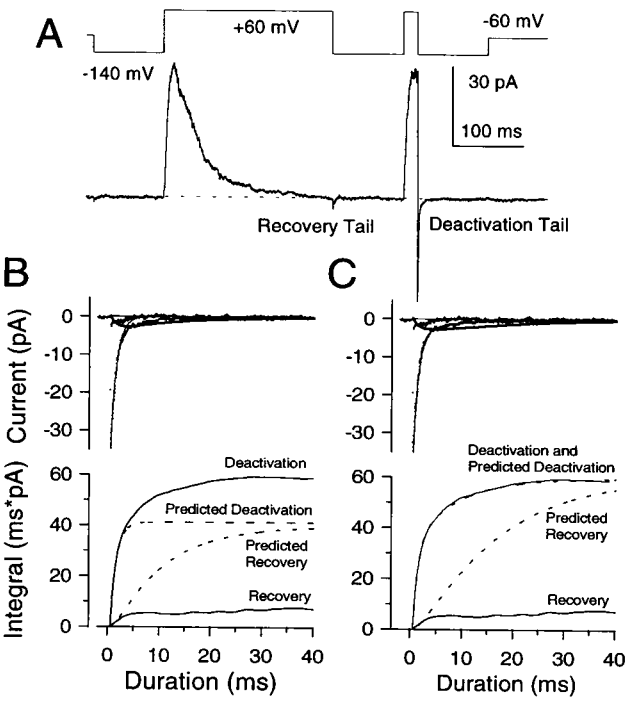

FIGURE 5 Inactivated BK_i channels recover from open states without significant passage through open states. (*A*) An inside-out patch was bathed with 10 μM submembrane Ca^{2+}. The voltage waveform shown on the top was used to elicit BK activity, and the resulting ensemble average is shown on the bottom. An idealization of traces without channel openings obtained in 0 Ca^{2+} were subtracted from each trace used to generate the ensemble (66 sweeps). The first 500 μs after each voltage step was nulled. (*B*) The top panel shows the aligned current records for the two repolarizations to −140 mV from +60 mV at larger amplification (points at 40 μs sampling). The solid line through the deactivation tail currents shows the best fit of a single exponential function (τ_i = 1.21 ms). Note that there is a second, slower exponential component, which is not used for calculation of expected slow tail current. The thickened line is the expectation for current that would occur during recovery from inactivation, if all inactivated channels must pass through the open before deactivating. This assumes a recovery rate of 80/s and a deactivation rate of 826/s. On the bottom, currents were digitally integrated to yield the deactivation and recovery current integrals. Predicted deactivation and predicted recovery traces were obtained from integration of the single-exponential deactivation decay and the predicted slow tail in the upper panel. Because the first 500 μs of the current relaxations was excluded from the tails and the integrals, all current integrals are underestimates of the actual integrals. (*C*) *Top:* Both deactivation and recovery tails are again plotted along with a two-exponential fit (τ_f = 1.03 ms; τ_s = 8.4 ms) to the deactivation time course. In this case, the thickened line shows the predicted slow tail current when both slow and fast deactivating channels are taken into account. *Bottom:* The observed and predicted deactivation and recovery current integrals are plotted as in *B*.

−140 mV removes most channels from inactivation. A subsequent, prolonged step to +60 mV results in activation of BK openings, which largely inactivate during the depolarizing step. A 100-ms step to −140 mV was then used to produce full recovery from inactivation and to define the tail of the current when all channels were inactivated at the time of repolarization. A subsequent 20-ms step to +60 mV demonstrates that all inactivated channels have recovered from inactivation, whereas the subsequent repolarization to −140 mV at the peak of current activation defines the tail current amplitude that results when all channels return to rest through the open state. The top panel of Fig. 5 *B* aligns the tail currents obtained at −140 mV for each of the two cases. The normal deactivation tail decays with a time constant of 1.21 ms (there is also a small second exponential component; see Solaro et al., 1995). There is only a small tail after repolarization after the inactivating step to +60 mV. Because raw currents were averaged for these traces, at least some of this tail is likely to reflect deactivation of other channels in the patch, including voltage-dependent K^+ channels.

We next wished to ascertain how much tail current would be expected during recovery from inactivation, assuming that all inactivated channels had to return to the resting condition by passing through open states. We have conservatively excluded currents during the first 500 μs after the repolarizing voltage step to ensure that no uncorrected capacitive currents bias the result. The consequences of this exclusion are considered below. Results above indicated that with symmetrical K^+, recovery from inactivation at −140 mV occurs at a rate of ~80–100/s. Using the peak of the deactivation tail to define the maximum current and assuming that channels recovering at a rate of 80/s first enter an open state before deactivating at a rate of 826/s, we would expect to observe a slow tail shown by the thickened line plotted in Fig. 5 *B*. Although the expected current is small, it has a notable rising phase. A current of this type was never observed in six patches. The bottom panel of Fig. 5 *B* displays the current integrals resulting from the two current averages and the idealized current. The current integral dramatically illustrates the difference in total open time between the two cases. Fig. 5 *C* extends this analysis to take into account both fast and slow components of the deactivation tail. Given the additional current contributed by the slow deactivation tail component, this predicts an even larger slow tail current during recovery from inactivation. Thus the absence of the predicted slow tail in the current averages after inactivation argues that recovery occurs without appreciable passage through open states.

In this analysis of tail currents associated with deactivation or after complete inactivation of BK current, we have omitted the first 500 μs after the voltage step from analysis. Therefore, the peak deactivation tail current after repolarization of open channels is underestimated. As a corollary, the amplitudes of the predicted slow tail current that would result from channels obligatorily reopening after recovery from inactivation (*thickened lines in the top panels* of Fig. 5, *B* and *C*) are also underestimated. Thus the differences between the predicted slow tails and those observed would be even larger than seen in Fig. 5, further supporting the idea that channels recovering from inactivation are unlikely to pass through an open state.

DISCUSSION

Summary

Despite some similarity between inactivation of BK_i channels in rat chromaffin cells and rapid inactivation of other voltage-dependent channels, the present experiments point out several important differences with other previously described inactivation mechanisms. Our earlier results have shown that BK_i inactivation involves multiple cytosolic trypsin-sensitive structures (Solaro and Lingle, 1992; Lingle et al., 1996). However, the present experiments with cytosolic blockers argue that inactivation does not result from movement of a blocking particle into a position that closely abuts the cytosolic mouth of the channel or from a channel constriction in the cytosolic half of the pore. Furthermore, in contrast to ball-and-chain type inactivation, recovery from inactivation occurs without appreciable passage of channels through an open state. Together, the lack of effect of cytosolic blockers and the absence of channel reopening during recovery from inactivation suggest that the barrier to ion permeation that results from inactivation is not closely associated with the pore or within the pore itself. Movement of the inactivation domain is apparently not hindered by occupancy of the cytosolic end of the pore. An additional implication is that conformational changes associated with channel closing can apparently occur in inactivated channels.

In contrast to the above view, however, the effects of extracellular K^+ might be used to argue that changes within the pore are important for inactivation. Specifically, the ability of the permeant extracellular ion, K^+, but not the impermeant ion, Na^+, to influence the inactivation process suggests that the block to permeation occurring during inactivation is sensitive to pore occupancy. One possibility might be that the barrier to permeation that occurs during inactivation is simply external to the internal Cs^+ blocking site. The difficulty with this view is explaining the effect of cytosolic trypsin on the inactivation process. An alternative way of explaining the effects of extracellular K^+ is to suppose that pore occupancy by permeant ions may simply favor a channel state from which recovery from inactivation is more likely. Irrespective of the way in which the various aspects of these results are resolved, together the results reveal that BK_i inactivation exhibits a set of mechanistic features that imply functional and structural differences from other previously described inactivation mechanisms.

Cytosolic blockers and inactivation

The inability of any cytosolic blocker to influence the normal inactivation rate suggests that the native BK_i inac-

tivation domains do not interact either sterically or electrostatically with even large molecules that bind to sites within or near the entrance to the ion permeation pathway. The dimensions of the blockers used here place some constraints on the closest approach distance of any putative inactivation domains to the pore. Estimates based on solvent free minimizations of the longest dimension for the blockers used in this study are listed in Table 1. Decamethonium may access its blocking position in a folded conformation (Miller, 1982; Villarroel et al., 1988), thus limiting the distance it extends from its blocking site. Based on estimates of electrical distance for blockade of BK channels using bisquaternary ammonium blockers (Villarroel et al., 1988), TEA or other quaternary ammonium moieties have been proposed to reside ~10 Å within the pore, assuming a uniform field through the membrane not altered by the presence of blocker itself. One difficulty with these earlier estimates of physical distance is the unanswered question of how both quaternary head groups in a molecule like decamethonium manage to occupy a similar electrical position within what is presumed to be a somewhat constricted space. Yet, ignoring this uncertainty about the physical distance between any blocking site and the actual entrance to the channel, the present results would only suggest that the native inactivation domain, if it is acting by occluding the channel, cannot approach closer than ~6–7 Å from the mouth of the ion permeation pathway (with the assumption that the quaternary moiety of the blockers resides ~10 Å into the field; Villarroel et al., 1988). Dependent upon how each blocker extends from the mouth of the channel, this minimal approach distance might be even less. The implications of the lack of effect of BP are less clear. BP has been proposed to adopt a β structure strongly favored by hydrophobic conditions (Fernandez-Ballester et al., 1995), although mammalian inactivation peptides appear to adopt a more ordered structure (Antz et al., 1997). Although a globular peptide of 22 amino acids would exclude a spherical volume of ~17.5 Å diameter (Creighton, 1993), when adopting a more extended β structure, depending on the orientation of the peptide, the peptide may extend either less or more than 17 Å from the entrance to the permeation pathway. With certain orientations, the limits defined by BP may not be too different from those defined by the quaternary blockers. Therefore, the geometric considerations suggest that occlusion may still be a plausible mechanism, but that the closest approach of the occluding structure to the mouth of the ion channel must be at a distance of perhaps 5–20 Å. This seems sufficiently small to imagine that a tight barrier to ion permeation could still arise at this distance. The recent structural study on mammalian inactivation peptides is of particular interest in this regard (Antz et al., 1997). Coupled with a model of *Shaker* channel structure (Guy and Durell, 1992), blockade by inactivation peptides can be seen to occur by entry of the peptides into a prolonged vestibule with subsequent binding and blockade at the mouth of the pore. The dimensions of the vestibule in this model (Antz et al., 1997) suggest that more superficial binding of peptides within the vestibule at sites unlikely to result in interactions with pore blockers may be plausible.

In contrast to the quaternary blockers, internal blockade by Cs^+ is thought to occur at a deeper site within the pore (Cecchi et al., 1987). This earlier work provides reasonable support for the idea that Cs^+ blockade involves action at a single site within the pore with an effective blocking valence, $z\delta$, of ~0.54 (Cecchi et al., 1987), whereas TEA block was described by a $z\delta$ of 0.27 (Villarroel et al., 1988). Work on bovine chromaffin cell BK channels suggested somewhat different positions of blockade by TEA and Cs^+, with $z\delta$ positions of 0.1 and 0.25, respectively (Yellen, 1984). However, in both sets of experiments, the results are consistent with Cs^+ blocking at a deeper position within the channel than TEA. Taken together then, the lack of effect of quaternary blockers and Cs^+ on BK_i inactivation lends support to the idea that the barrier to ion permeation during BK_i inactivation does not occur within the half of the pore most accessible from the cytosol.

The lack of reopening during recovery from inactivation

The present results indicate that, during recovery from inactivation, most channels recover to resting states without passing through an open state. An implication of this result is that those channels that recover without opening must therefore be able to deactivate while inactivated. Thus, while in the inactivated conformation, the gate involved in the movement from open to closed is apparently not impeded by the native inactivation domain. However, one is then left with the difficulty of how to explain both the apparent coupling of inactivation rate to channel activation (Solaro and Lingle, 1992; Prakriya et al., 1996) and the fact that recovery from inactivation is faster at lower Ca^{2+} and more negative potentials (Herrington et al., 1995; Ding et al., 1996). These latter features of inactivation would imply that the blocking mechanism and/or particle requires that some sort of conformational change associated with channel gating favor the inactivated condition. Yet, because inactivation does not impede the normal deactivation process, the results suggest that opening per se may also not be required for inactivation. Because the lack of effect of blockers suggests that inactivation is unlikely to involve direct binding at either end of the pore, one must then posit conformational changes outside the pore associated with channel activation that are critical for the inactivation process to occur.

Effects of extracellular ions on inactivation

The dependence of recovery from inactivation on extracellular $[K^+]_o$ is similar to that previously observed for recovery from inactivation of *Shaker* K^+ channels (Demo and Yellen, 1991) and for dissociation of the *Shaker* BP from the *Shaker* B channel (Murrell-Lagnado and Aldrich, 1993).

Although blockade by BP of BK channels has also been shown to be dependent on changes in extracellular K^+ (Foster et al., 1992; Toro et al., 1992), there is some dispute about whether BP association or dissociation is altered by increases in $[K^+]_o$. Although it is possible that the increase in BK_i recovery rate with increases in extracellular $[K^+]_o$ may reflect an interaction between K^+ and the native inactivation domain, other possibilities cannot be excluded. For example, BK channels are multiion pores with exceedingly complex interactions between occupancies of different sites (Neyton and Miller, 1988a,b; Neyton and Pelleschi, 1991). Furthermore, occupancy of BK channels and other voltage-dependent K^+ channels by ions is known to affect the stability of open and/or closed states (Neyton and Pelleschi, 1991; Demo and Yellen, 1992), which may indirectly influence inactivation kinetics. Although either of these two alternative explanations could be used to reconcile the lack of effect of cytosolic blockers on inactivation onset with the results with extracellular $[K^+]$, changes in extracellular $[K^+]$ are not thought to influence the closed-open equilibrium of BK channels (Neyton and Pelleschi, 1991; Demo and Yellen, 1992). Thus a more systematic examination of the effects of different cations on inactivation kinetics and gating equilibrium will be required to illuminate this issue. However, whatever the mechanism of K^+ action, the lack of effect of Na^+ on recovery rate suggests that the effects of K^+ probably reflect occupancy by K^+ of a site within the pore. Two external ion-binding sites within the BK channel have been proposed to participate in influencing Ba^{2+} binding at an internal site (Neyton and Miller, 1988a). Occupancy of the so-called external lock-in (ELI) site by Na^+, albeit at low affinity (30–60 mM; Neyton and Miller, 1988a; Neyton and Pelleschi, 1991), or K^+, at much higher affinity (200–300 μM; Neyton and Miller, 1988b; Neyton and Pelleschi, 1991), slows Ba^{2+} dissociation from its internal blocking site. A more internal site, called the enhancement site, promotes dissociation of internal Ba^{2+} (Neyton and Miller, 1988b). Both the lack of effect of Na^+ and the apparent EC_{50} for the effect of $[K^+]_o$ on recovery ($\sim$111 mM) would be generally consistent with the expected properties of the internal enhancement site, suggesting that this site may influence recovery from inactivation. However, it must be considered that previous estimates of K^+ affinities for both the ELI site and the enhancement site were determined solely within the context of Ba^{2+} occupancy of the internal Ba^{2+} blocking site.

Evaluation of any effect of external K^+ on an unknown inactivation process must also consider the fact that recovery from C-type inactivation is also faster with increases in $[K^+]_o$ (Levy and Deutsch, 1996). Thus our results obtained with extracellular K^+ do not provide direct information about the location or arrangement of inactivation gates and channel occupancy by ions. Given the evidence suggesting that inactivation involves a cytosolic, trypsin-sensitive structure that does not appear to interact directly with the mouth of the channel, we suggest that occupancy of the pore by K^+ does not increase the recovery rate by a direct electrostatic interaction with the inactivation domain, but rather favors a channel conformation favorable to recovery from inactivation.

It has been proposed that the voltage dependence of recovery from the inactivation of *Shaker* B channels may arise because of the voltage dependence of occupancy of the permeation pathway by permeant ions (Demo and Yellen, 1991). Our results indicated that, in several different solutions, each with 0 extracellular permeant ions, recovery from inactivation retained voltage dependence, although it was reduced relative to that with more elevated $[K^+]_o$. The residual voltage dependence may reflect either the voltage dependence of dissociation of a native inactivation domain or, alternatively, reflect the voltage dependence of the equilibrium of a state favorable for recovery from inactivation.

Speculations about inactivation mechanisms

The ability of trypsin to abolish inactivation (Solaro and Lingle, 1992) requires that some structure, essential to the inactivation process, be located on the cytosolic face of the channel. The results provide no direct evidence that a trypsin-sensitive cytosolic structure actually occludes access of ions to the permeation pathway. It might be argued that the structural change associated with inactivation occurs within the permeation pathway or even on the extracellular face, but that this structural change is somehow coupled to trypsin-sensitive residues on the cytosolic face of the channel. Because of evidence suggesting that the barrier to permeation during inactivation is not within the inner half of the pore, we think this possibility is not likely.

If the barrier to ion permeation resulting from inactivation is neither within the pore itself or at the ends of the pore, where can this barrier be? Given the absence of evidence in support of an occlusion mechanism, we must at least consider the possibility that some entirely different type of mechanism is responsible for BK_i inactivation. For example, perhaps there is no cytosolic blocking structure, but inactivation results simply from normal deactivation of the channel that occurs after some change in the ability of Ca^{2+} to gate the channel. The lack of reopenings during the recovery from inactivation might be consistent with this idea, because a channel would simply remain deactivated as the ability of Ca^{2+} to gate the channel was restored. Furthermore, trypsin might simply alter the ability of some cytosolic domain to interfere with Ca^{2+}-dependent gating. However, if the conformational change within the pore associated with inactivation were identical to that occurring during deactivation, manipulations that alter the normal deactivation process (e.g., ions or blockers) would also be expected to influence inactivation. Although additional experiments will be required to fully address this issue, the results, which suggest that BK_i inactivation is not associated with a constriction or block to ion permeation within the pore, also argue that inactivation is structurally different from the conformational change associated with deactiva-

tion. Despite the fact that there is no direct evidence that BK_i inactivation domains occlude access of permeant ions to the channel entrance, we feel this remains the most plausible view. However, in contrast to *Shaker*-type ball-and-chain inactivation, the inactivation domains occupy a position of occlusion that does not abut the mouth of the ion channel. Irrespective of the exact physical picture by which inactivation may occur, these results demonstrate that inactivation of chromaffin cell BK channels probably does not involve a typical direct channel-blocking interaction of an inactivation domain with the mouth of the ion permeation pathway.

The molecular components required for inactivation

The present results provide no information about whether the structure required for inactivation is intrinsic to the main channel protein or part of an accessory protein that may associate with the channel. Recently, an interesting 59-amino acid insert encoded by a novel exon has been identified in *Slo* homologs from chromaffin cells (Saito et al., 1997). Although the 59-amino acid insert encoded by a novel alternative splice variant does not confer inactivation on *Slo* constructs when expressed in *Xenopus* oocytes (Saito et al., 1997), this variant is also found in rat pancreatic β cells, another cell in which inactivating variants of BK channel have been identified (Lingle et al., 1996). This suggests that this exon may be a unique component of inactivating BK channels, perhaps anchoring interaction with a domain or protein that is essential for inactivation.

This work was supported by DK-46564 from the National Institutes of Health.

REFERENCES

Antz, C., M. Geyer, B. Fakler, M. K. Schott, H. R. Guy, R. Frank, J. P. Ruppersberg, and H. R. Kalbitzer. 1997. NMR structure of inactivation gates from mammalian voltage-dependent potassium channels. *Nature.* 385:272–275.

Cecchi, X., D. Wolff, O. Alvarez, and R. Latorre. 1987. Mechanisms of Cs^+ blockade in a Ca^{2+}-activated K^+ channel from smooth muscle. *Biophys. J.* 52:707–716.

Choi, K. L., R. W. Aldrich, and G. Yellen. 1991. Tetraethylammonium blockade distinguishes two inactivation mechanisms in voltage-activated K^+ channels. *Proc. Natl. Acad. Sci. USA.* 88:5092–5095.

Covarrubias, M., A. Wei, L. Salkoff, and T. B. Vyas. 1994. Elimination of rapid potassium channel inactivation by phosphorylation of the inactivation gate. *Neuron.* 13:1403–1412.

Creighton, T. E. 1993. Proteins: Structures, and Molecular Properties, 2nd Ed. W. H. Freeman, New York.

Demo, S. D., and G. Yellen. 1991. The inactivation gate of the *Shaker* K^+ channel behaves like an open-channel blocker. *Neuron.* 7:743–753.

Demo, S. D., and G. Yellen. 1992. Ion effects on gating of the Ca^{2+}-activated K^+ channel correlate with occupancy of the pore. *Biophys. J.* 61:639–648.

Ding, J. P., C. R. Solaro, and C. J. Lingle. 1996. The dependence of recovery from inactivation of BK channels in rat chromaffin cells on calcium and voltage. *Biophys. J.* 70:A192.

England, S. K., V. N. Uebele, H. Shear, J. Kodali, P. B. Bennett, and M. M. Tamkun. 1995. Characterization of a voltage-gated K^+ channel β subunit expressed in human heart. *Proc. Natl. Acad. Sci. USA.* 92: 6309–6313.

Fernandez-Ballester, G., F. Gavilanes, J. P. Albar, M. Criado, J. A. Ferragut, and J. M. Gonzalez-Ros. 1995. Adoption of β structure by the inactivating "ball" peptide of the *Shaker* B potassium channel. *Biophys. J.* 68:858–865.

Foster, C. D., S. Chung, W. N. Zagotta, R. W. Aldrich, and I. B. Levitan. 1992. A peptide derived from the *Shaker* B K^+ channel produces short and long blocks of reconstituted $Ca^{(2+)}$-dependent K^+ channels. *Neuron.* 9:229–236.

Gomez-Lagunas, F., and C. M. Armstrong. 1994. The relation between ion permeation and recovery from inactivation of *Shaker*B K^+ channels. *Biophys. J.* 67:1806–1815.

Gomez-Lagunas, F., and C. M. Armstrong. 1995. Inactivation in *Shaker*B K^+ channels: a test for the number of inactivating particles on each channel. *Biophys. J.* 68:89–95.

Gonoi, T., and B. Hille. 1987. Gating of Na Channels. Inactivation modifiers discriminate among models. *J. Gen. Physiol.* 89:253–274.

Guy, H. R., and S. R. Durell. 1992. Atomic scale structure and functional models of voltage-gated potassium channels. *Biophys. J.* 62:238–250.

Hamill, O. P., A. Marty, E. Neher, B. Sakmann, and F. J. Sigworth. 1981. Improved patch clamp techniques for high-resolution current recording from cells and cell-free membrane patches. *Pflügers Arch.* 391:85–100.

Herrington, J., C. R. Solaro, A. Neely, and C. J. Lingle. 1995. Suppression of calcium- and voltage-activated current by muscarinic acetylcholine receptor activation in rat chromaffin cells. *J. Physiol. (Lond.).* 485: 297–318.

Hodgkin, A. L., and A. F. Huxley. 1952. A quantitative description of membrane current and its application to conduction and excitation in nerve. *J. Physiol. (Lond.).* 117:500–544.

Hoshi, T., W. N. Zagotta, and R. W. Aldrich. 1990. Biophysical and molecular mechanisms of *Shaker* potassium channel inactivation. *Science.* 250:533–538.

Hoshi, T., W. N. Zagotta, and R. W. Aldrich. 1991. Two types of inactivation in *Shaker* K^+ channels: effects of alterations in the carboxy-terminal region. *Neuron.* 7:547–556.

Jerng, H. H., and M. Covarrubias. 1997. K^+ channel inactivation mediated by the concerted action of the cytoplasmic N- and C-terminal domains. *Biophys. J.* 72:163–174.

Kuo, C.-C., and B. P. Bean. 1994. Na^+ channels must deactivate to recover from inactivation. *Neuron.* 12:819–829.

Levy, D. I., and C. Deutsch. 1996. Recovery from C-type inactivation is modulated by extracellular potassium. *Biophys. J.* 70:798–805.

Lingle, C. J., C. R. Solaro, M. Prakriya, and J. P. Ding. 1996. Calcium-activated potassium channels in adrenal chromaffin cells. *In* Ion Channels, Vol. 4. T. Narahashi, editor. Plenum Press, New York.

Lopez-Barneo, J., T. Hoshi, S. H. Heinemann, and R. W. Aldrich. 1993. Effects of external cations and mutations in the pore region on C-type inactivation of *Shaker* potassium channels. *Recept. Channels.* 1:61–71.

MacKinnon, R. 1991. Determination of the subunit stoichiometry of a voltage-activated potassium channel. *Nature.* 350:232–235.

MacKinnon, R., R. W. Aldrich, and A. W. Lee. 1993. Functional stoichiometry of *Shaker* potassium channel inactivation. *Science.* 262:757–759.

Matteson, D. R., and R. P. Swenson. 1986. External monovalent cations that impede the closing of K^+ channels. *J. Gen. Physiol.* 87:795–816.

Miller, C. 1982. Bis-quaternary ammonium blockers as structural probes of the sarcoplasmic reticulum K^+ channel. *J. Gen. Physiol.* 79:869–891.

Morales, M. J., R. C. Castellino, A. L. Crews, R. L. Rasmusson, and H. C. Strauss. 1995. A novel β subunit increases rate of inactivation of specific voltage-gated potassium channel α subunits. *J. Biol. Chem.* 270: 6272–6277.

Murrell-Lagnado, R. D., and R. W. Aldrich. 1993. Energetics of *Shaker* K channels block by inactivation peptides. *J. Gen. Physiol.* 102:977–1003.

Neely, A., and C. J. Lingle. 1992. Two components of calcium-activated potassium current in rat adrenal chromaffin cells. *J. Physiol. (Lond.).* 453:97–131.

Neyton, J., and C. Miller. 1988a. Potassium blocks barium permeation through a calcium-activated potassium channel. *J. Gen. Physiol.* 92: 549–567.

Neyton, J., and C. Miller. 1988b. Discrete Ba^{2+} block as a probe of ion occupancy and pore structure in the high-conductance Ca^{2+}-activated K^+ channels. *J. Gen. Physiol.* 92:569–586.

Neyton, J., and M. Pelleschi. 1991. Multi-ion occupancy alters gating in high-conductance, Ca^{2+}-activated K^+ channels. *J. Gen. Physiol.* 97: 641–665.

Oda, M., A. Yoshida, and Y. Ikemoto. 1992. Blockade by local anaesthetics of the single Ca^{2+}-activated K^+ channel in rat hippocampal neurones. *Br. J. Pharmacol.* 105:63–70.

Ogielska, E. M., W. N. Zagotta, T. Hoshi, S. H. Heinemann, J. Haab, and R. W. Aldrich, 1995. Cooperative subunit interaction in C-type inactivation of K^+ channels. *Biophys. J.* 69:2449–2457.

Panyi, G., Z. Sheng, L. Tu, and C. Deutsch. 1995. C-type inactivation of a voltage-gated K^+ channel occurs by a cooperative mechanism. *Biophys. J.* 69:896–903.

Patton, D. E., J. W. West, W. A. Catterall, and A. L. Goldin. 1993. A peptide segment critical for sodium channel inactivation functions as an inactivation gate in a potassium channel. *Neuron.* 11:967–974.

Prakriya, M., C. R. Solaro, J. P. Ding, and C. J. Lingle. 1996. $[Ca^{2+}]_i$ elevations detected by BK channels during Ca^{2+} influx and muscarine-mediated release of Ca^{2+} from intracellular stores in rat chromaffin cells. *J. Neurosci.* 16:4344–4359.

Rettig, J., S. H. Heinemann, F. Wunder, C. Lorra, D. N. Parcej, J. O. Dolly, and O. Pongs. 1994. Inactivation properties of voltage-gated K^+ channels altered by the presence of β-subunit. *Nature.* 369:289–294.

Rojas, E., and C. M. Armstrong. 1971. Sodium conductance activation without inactivation in pronase-perfused axons. *Nature New Biol.* 229: 177–178.

Ruppersberg, J. P., R. Frank, O. Pongs, and M. Stocker. 1991. Cloned neuronal $I_K(A)$ channels reopen during recovery from inactivation. *Nature.* 353:657–660.

Saito, M., C. Nelson, L. Salkoff, and C. J. Lingle. 1997. A cysteine-rich domain defined by a novel exon in a *Slo* variant in rat adrenal chromaffin cells and PC12 cells. *J. Biol. Chem.* 272:11710–11717.

Shen, K. Z., A. Lagrutta, N. W. Davies, N. B. Standen, J. P. Adelman, and R. A. North. 1994. Tetraethylammonium block of slowpoke calcium-activated potassium channels expressed in *Xenopus* oocytes: evidence for tetrameric channel formation. *Pflügers Arch.* 426:440–445.

Solaro, C. R., and C. J. Lingle. 1992. Trypsin-sensitive, rapid inactivation of a calcium-activated potassium channel. *Science.* 257:1694–1698.

Solaro, C. R., M. Prakriya, J. P. Ding, and C. J. Lingle. 1995. Inactivating and non-inactivating Ca^{2+} and voltage-dependent K^+ current in rat adrenal chromaffin cells. *J. Neurosci.* 15:6110–6123.

Toro, L., E. Stefani, and R. Latorre. 1992. Internal blockade of a Ca^{2+}-activated K^+ channel by *Shaker* B inactivating "ball" peptide. *Neuron.* 9:237–245.

Vassilev, P. M., T. Scheuer, and W. A. Catterall. 1988. Identification of an intracellular peptide segment involved in sodium channel inactivation. *Science.* 241:1658–1661.

Villarroel, A., O. Alvarez, A. Oberhauser, and R. Latorre. 1988. Probing a Ca^{2+}-activated K^+ channel with quaternary ammonium ions. *Pflügers Arch.* 413:118–126.

Yellen, G. 1984. Ionic permeation and blockade in Ca^{2+}-activated K^+ channels of bovine chromaffin cells. *J. Gen. Physiol.* 84:157–186.

Zagotta, W. N., T. Hoshi, and R. W. Aldrich. 1990. Restoration of inactivation in mutants of *Shaker* potassium channels by a peptide derived from ShB. *Science.* 250:568–571.